

Why do dusk-active cockchafers detect polarization in the green? The polarization vision in *Melolontha melolontha* is tuned to the high polarized intensity of downwelling light under canopies during sunset

Ramón Hegedüs^a, Ákos Horváth^b, Gábor Horváth^{a,*}

^aBiooptics Laboratory, Department of Biological Physics, Loránd Eötvös University, H-1117 Budapest, Pázmány Péter sétány 1, Hungary

^bJet Propulsion Laboratory, California Institute of Technology, 4800 Oak Grove Drive, Pasadena, California, 91109, USA

Received 23 March 2005; received in revised form 10 May 2005; accepted 10 May 2005

Available online 25 July 2005

Abstract

In the retina of dusk-active European cockchafers, *Melolontha melolontha*, the linear polarization of downwelling light (skylight or light from the tree canopy) is detected by photoreceptors in upward-pointing ommatidia with maximal sensitivity at 520 nm in the green portion of the spectrum. To date no attempt has been made to answer the question of why these beetles detect polarization in the green. Here we present an atmospheric optical and receptor-physiological explanation of why longer wavelengths are advantageous for the perception of polarization of downwelling light under canopies illuminated by the setting sun. Our explanation focuses on illumination situations during sunset in canopied optical environments, because cockchafers are active at sunset and fly predominantly under canopies during their swarming, feeding, and mating periods. Using three simple atmospheric optical models, we computed the degree of linear polarization, the linearly polarized intensity of downwelling light, the quantum catch, and quantum catch difference between polarization detectors with orthogonal microvilli under canopies illuminated by the setting sun as functions of wavelength and solar zenith angle. Based upon these computations, we show that the green sensitivity of polarization detectors in *M. melolontha* is tuned to the high polarized intensity of downwelling light in the green under canopies during sunset, an optimal compromise between simultaneous maximization of the quantum catch and the quantum catch difference. We also briefly discuss how green-sensitive polarization detectors can function efficiently enough during the pre-feeding and egg-laying flights of cockchafers, which always occur prior to sunset and under the sky.

© 2005 Elsevier Ltd. All rights reserved.

Keywords: European cockchafer; *Melolontha melolontha*; Polarization vision; Dusk activity; Sunset light; Canopylight; Green sensitivity; Downwelling light

1. Introduction

In insects, the linear polarization of downwelling light (skylight or light from the tree canopy) is detected by upward-pointing ommatidia in the so-called dorsal rim area (DRA) of the compound eye. These ommatidia are anatomically and physiologically specialized, and contain two sets of monochromatic and highly polarization-

sensitive photoreceptors with orthogonal microvilli directions (Labhart and Meyer, 1999). The spectral type of the DRA receptors is ultraviolet (UV) in flies, honeybees, desert ants, certain scarab beetles, and spiders while being blue in crickets, desert locusts, and cockroaches (Table 10.1 of Horváth and Varjú, 2003; Table 1 of Barta and Horváth, 2004).

Explanations for cricket preference of the blue part of the spectrum for detection of skylight polarization have been discussed qualitatively by Labhart et al. (1984), Herzmann and Labhart (1989), Zufall et al. (1989),

*Corresponding author. Tel.: +36 1 372 2765; fax: +36 1 372 2757.
E-mail address: gh@arago.elte.hu (G. Horváth).

Horváth and Varjú (2003), and Barta and Horváth (2004). The cricket *Gryllus campestris* is active not only during the day, but also during crepuscular periods (dusk and dawn) and at night, having highly polarization-sensitive blue receptors in its DRA. Horváth and Varjú (2003) and Barta and Horváth (2004) showed that the degree of linear polarization p_{cloudy} of light from cloudy parts of the sky is always relatively high in the violet and blue ($400\text{ nm} < \lambda < 470\text{ nm}$), rendering the violet-blue the second optimal spectral range after the UV (in which p_{cloudy} is maximal) for detection of skylight polarization under partly cloudy conditions. Using the blue portion of the spectrum at twilight has a significant advantage over using UV under clear skies, when the degree of skylight polarization is sufficiently high for all wavelengths (Fig. 1A). The intensity I of the UV component of sunlight (Fig. 1B,C) and light from the clear sky is low relative to that of the blue and green components. At twilight under clear sky, the light intensity is more likely to fall below the sensitivity threshold of a polarization-sensitive visual system operating in the UV rather than in the blue. According to Zufall et al. (1989), the combination of blue spectral and polarization sensitivity in the DRA may be a common adaptation of insects that are active at circumstances of very low light intensities, as opposed to day-active insects (e.g. honeybees, desert ants, and flies) which predominantly use UV receptors as detectors for skylight polarization (see Table 10.1 of Horváth and Varjú, 2003, p. 54). However, the question is whether this argument also holds for cloudy conditions. On the one hand, detection of skylight may be more disadvantageous in the UV than in the blue, because under cloudy conditions the UV component of skylight is weaker than the blue component. On the other hand, perception of skylight polarization could be more advantageous in the UV than in the blue, because under cloudy skies p_{cloudy} is the highest in the UV (see Fig. 4 of Barta and Horváth, 2004). The question is, which effect is the stronger one.

The perception of skylight polarization in the UV by several insect species is surprising, because both the degree of linear polarization p (Fig. 1A), and the intensity I (Fig. 1B, C) of light from the clear sky are considerably lower in the UV than in the blue or green. This is called the “UV-sky-pol paradox”. Although in the past several attempts have been made to resolve this paradox, none of them has been convincing, as Horváth and Varjú (2003) and Barta and Horváth (2004) have shown. Horváth and Varjú (2003) and Barta and Horváth (2004) have presented a quantitative resolution to the paradox. They have proved by model calculations that if the air layer between a cloud and a ground-based observer is partly sunlit at higher solar elevations, p of skylight originating from the cloudy region is highest in the UV (see Fig. 4 of Barta and Horváth, 2004), because

in this spectral range the unpolarized UV-deficient cloudlight dilutes the polarized light scattered in the air beneath the cloud the least. Similarly, if the air under foliage is partly illuminated by a high sun, p of downwelling light from the canopied region is maximal in the UV (see Fig. 5 of Barta and Horváth, 2004), because in this spectral range the unpolarized UV-deficient green canopylight dilutes the polarized light scattered in the air beneath the canopy the least. Therefore, in daylight the detection of polarization of downwelling light under clouds or canopies is most advantageous in the UV, in which spectral range the risk is smallest that p is lower than the threshold p_{tr} of polarization sensitivity in animals. On the other hand, under clear skies there is no favoured wavelength λ for perception of celestial polarization, because p of skylight is sufficiently high ($p > p_{tr}$) at all wavelengths. Horváth and Varjú (2003), and Barta and Horváth (2004) have also shown that there is an analogy between the detection of UV skylight polarization and the polarotactic water detection in the UV.

The aforementioned atmospheric optical reasons have provided researchers with a satisfying explanation for why certain insects detect the polarization of downwelling light either in the UV or in the blue part of the spectrum. However, there are at least two insect species in which the DRA receptors are green sensitive: In the retina of the European cockchafer, *Melolontha melolontha*, polarization is detected by receptors with maximal sensitivity at $\lambda_{max} = 520\text{ nm}$ (Labhart et al., 1992), and in the tenebrionid desert beetle, *Parastizopus armaticeps*, at $\lambda_{max} = 540\text{ nm}$ (Bisch, 1999). Why do these beetles detect polarization in the green? No attempt has been made to answer this question to date.

In this work, we present an atmospheric optical and receptor-physiological model to explain why longer wavelengths (green and red) are advantageous in the perception of the polarization of downwelling light under canopies illuminated by the setting sun. Our explanation focuses on illumination situations in a canopied optical environment at sunset, because cockchafers are active at dusk and fly predominantly under canopies during their swarming, feeding, and mating periods (Schneider, 1952). Using three simple atmospheric optical models, we compute the degree of linear polarization and the linearly polarized intensity of downwelling light, and the quantum catch and quantum catch difference between polarization detectors with orthogonal microvilli under canopies illuminated by sunlight as a function of the wavelength λ and the solar zenith angle θ . Based on these computations, we show that the green sensitivity of the polarization detectors in *M. melolontha* is tuned to the high polarized intensity of downwelling light in the green resulting in an optimal compromise between simultaneous maximization of the quantum catch and the quantum catch difference under

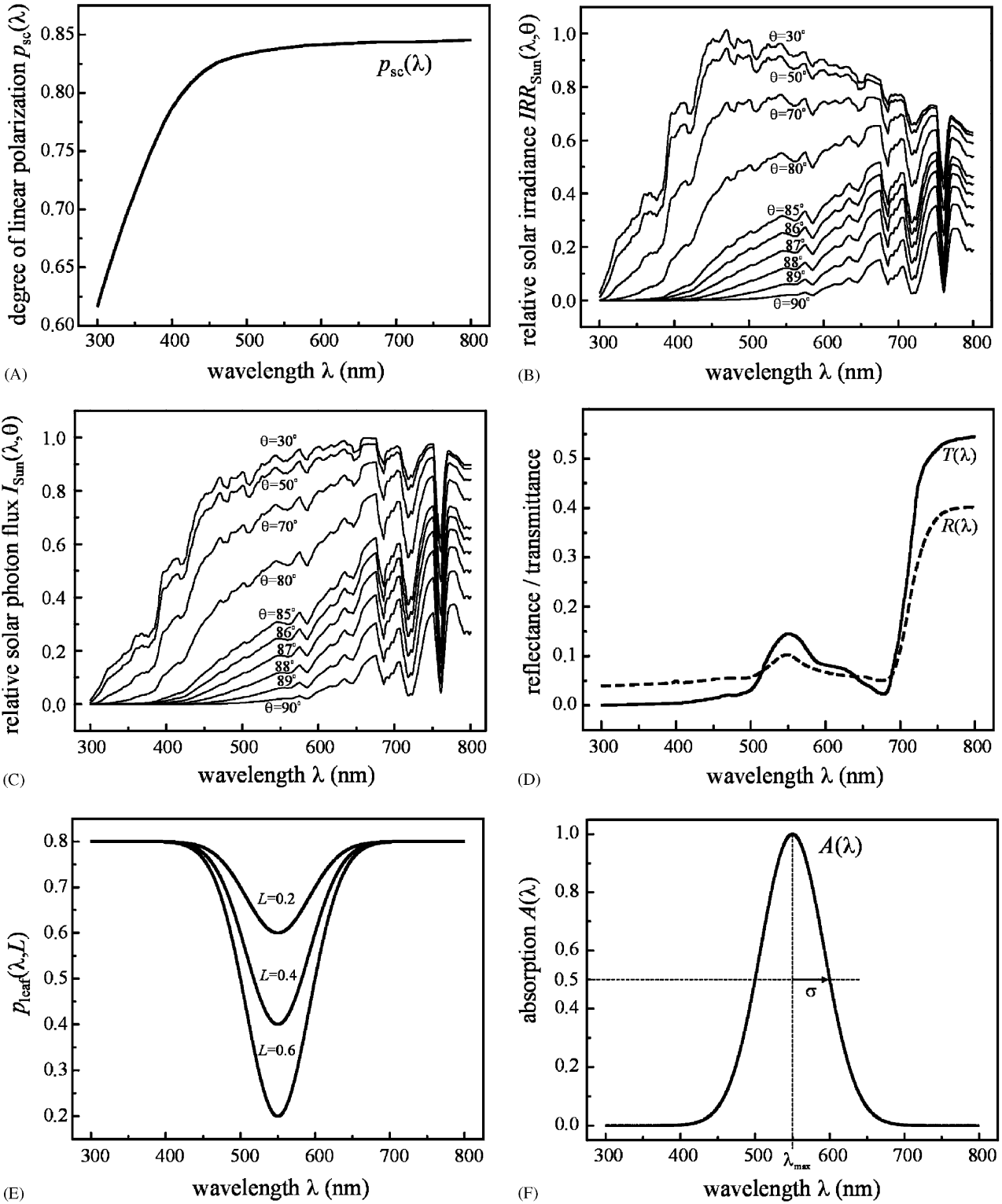


Fig. 1. (A) Degree of linear polarization p_{sc} versus wavelength λ of scattered light from clear sky measured at 90° from the sun, for a solar zenith angle $\theta = 80^\circ$ (Coulson, 1988, p. 285). (B) Relative irradiance $IRR_{Sun}(\lambda, \theta)$ of the unpolarized direct sunlight for solar zenith angles $\theta = 30^\circ, 50^\circ, 70^\circ, 80^\circ, 85^\circ, 86^\circ, 87^\circ, 88^\circ, 89^\circ$, and 90° (top to bottom), computed on the basis of the 1976 US Standard Atmosphere. (C) Relative solar photon flux $I_{Sun}(\lambda, \theta)$ for solar zenith angles $\theta = 30^\circ, 50^\circ, 70^\circ, 80^\circ, 85^\circ, 86^\circ, 87^\circ, 88^\circ, 89^\circ, 90^\circ$ (top to bottom). (D) Spectra of the reflectance $R(\lambda)$ and transmittance $T(\lambda)$ of cottonwood (*Populus deltoides*) leaves (Gates, 1980, p. 216). (E) Degree of linear polarization $p_{leaf}(\lambda, L)$ of light reflected from a green leaf calculated from Eq. (8) for $K = 0.8$, $\lambda_{min} = 550$ nm, $\sigma = 50$ nm, and $L = 0.2, 0.4, 0.6$. (F) Absorption spectrum $A(\lambda)$ of our model photoreceptor with maximal sensitivity at λ_{max} and bandwidth $\sigma = 50$ nm.

canopies during sunset. We briefly discuss why green-sensitive polarization detectors also function efficiently enough during the pre-feeding and egg-laying flights of cockchafers always occurring prior to sunset and under the sky. Finally, we explain qualitatively why the green-sensitive polarization detectors in *P. armaticeps* can also function efficiently enough at twilight under clear desert skies.

2. Materials and methods

2.1. Calculation of the degree of linear polarization and linearly polarized intensity of downwelling light under canopies illuminated by sunlight versus wavelength and solar zenith angle

Brines and Gould (1982), Pomozi et al. (2001), and Suhai and Horváth (2004) have experimentally shown that under frequently occurring illumination conditions the E-vector (or direction or angle of polarization) pattern of clouded celestial regions is approximately the same as that of the corresponding clear sky regions. Pomozi et al. (2001) have also demonstrated that in the visible part of the spectrum under partly cloudy conditions, the shorter the wavelength λ , the greater the proportion k of the celestial polarization pattern suitable for animal orientation. Hence, k is determined primarily by the degree of linear polarization p of skylight, for which Barta and Horváth (2004) have presented a quantitative estimation. They have also proposed that the E-vector pattern under canopies illuminated by sunlight should be nearly the same as that under clear sky at the same solar position. Consequently, p of downwelling light under canopy is what determines k . However, because the detectability of light polarization also depends on intensity I , the linearly polarized intensity $PI = pI$ also has to be taken into account in the estimation of the spectral region that is optimal for orientation by means of the polarization of downwelling light under canopies.

In this work we followed an atmospheric optical approach similar to Horváth and Varjú (2003) and Barta and Horváth (2004) in order to calculate the degree of linear polarization $p(\lambda)$ of downwelling light under canopies. We also computed the polarized intensity $PI(\lambda)$ and improved the model by investigating both $p(\lambda)$ and $PI(\lambda)$ as functions of the solar zenith angle θ ranging from 0° (sun at the zenith) to 90° (sun on the horizon). We focused on high values of θ , because cockchafers are active at dusk.

The at-ground direct-normal spectral solar irradiance, $IRR_{Sun}(\lambda, \theta)$, was simulated by MODTRAN (MODerate resolution TRANsmittance code) version 3.7 (Berk et al., 1983). MODTRAN includes a number of high-

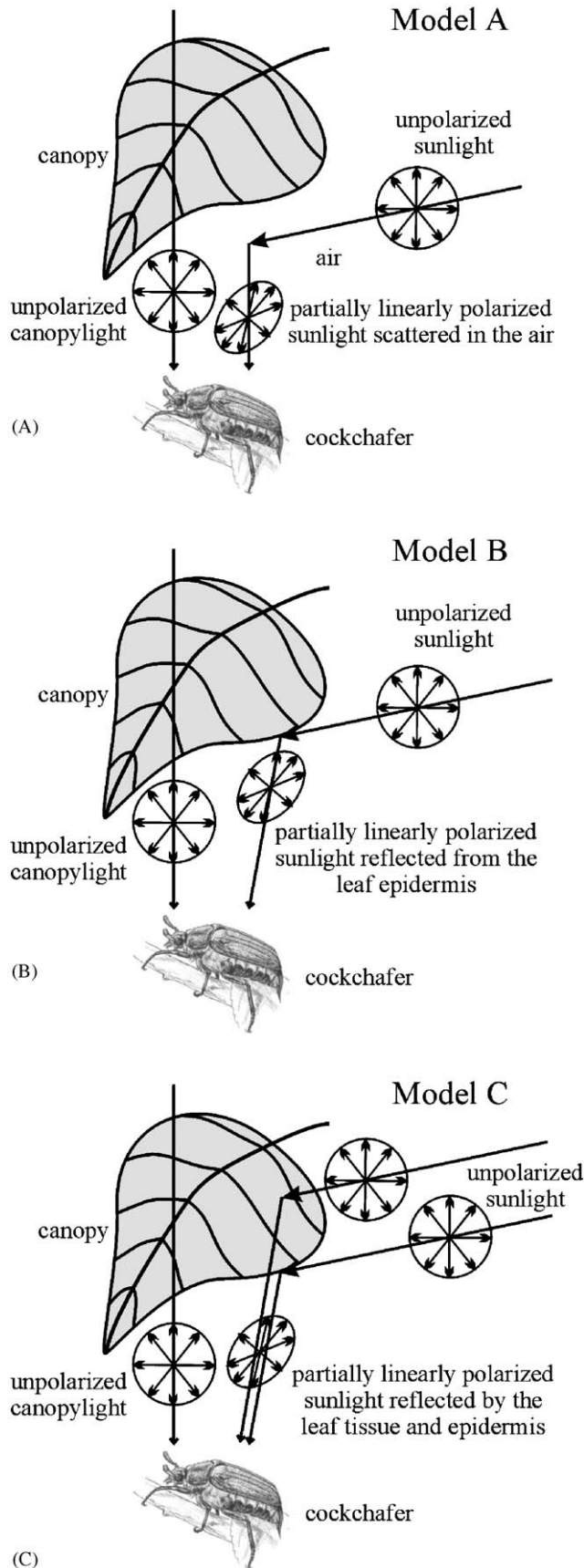
resolution (1 cm^{-1}) solar databases that differ from each other by only a couple of percent. The particular exo-atmospheric solar irradiance spectrum used in our calculations was based on the work of Kurucz (1995), Cebula et al. (1996), and Chance and Spurr (1997) and had a solar constant of 1362.12 W/m^2 . Spherical refraction and earth curvature (ray bending) were considered in the MODTRAN calculation of the atmospheric slant path and attenuation amounts along the path. In the absence of representative measurement data for the simulations, the vertical atmospheric profiles (of temperature, water vapour, ozone, etc.) were specified by the 1976 US Standard Atmosphere (COESA, 1976). This standard model describes an idealized steady-state atmosphere under moderate solar activity. The mixing ratio of CO_2 was set to 355 ppmv, and no aerosols, clouds, and rain were included in the simulations. The calculated at-ground solar irradiance spectrum was smoothed by convolution with a 5 nm wide square band kernel and tabulated at each 0.5 nm. The resulting solar irradiance spectrum is plotted in Fig. 1B for various solar zenith angles. As shown by Halthore et al. (1997), and Barducci et al. (2004), MODTRAN simulations of this kind are in very good agreement with measurements, provided the vertical atmospheric profiles are specified correctly.

The solar irradiance spectrum $IRR_{Sun}(\lambda, \theta)$ gives the energy of solar radiation per unit time, per unit area, per unit wavelength interval. However, photoreceptors respond to photon flux rather than photon energy, therefore, it is the number of photons and not the energy of the stimulating light that is important. Thus, $IRR_{Sun}(\lambda, \theta)$ was converted to solar photon flux $I_{Sun}(\lambda, \theta) = \lambda IRR_{Sun}(\lambda, \theta) / hc$, where h is the Planck constant and c is the velocity of light. $I_{Sun}(\lambda, \theta)$ gives the number of photons of solar radiation per unit time, per unit area, per unit wavelength interval, and is called the intensity of sunlight further on in this work (Fig. 1C).

In our models, the downwelling light under canopies illuminated by direct sunlight with spectrum $I_{Sun}(\lambda, \theta)$ had two components (Fig. 2). The first component, the unpolarized green canopylight transmitted through the foliage, was the same in all three models. The models differed only in the second component describing different polarized parts of the downwelling light under various illumination conditions. For all three models the wavelength range was $300 \text{ nm} \leq \lambda \leq 700 \text{ nm}$, including the UV ($300 \text{ nm} \leq \lambda \leq 400 \text{ nm}$) and visible ($400 \text{ nm} < \lambda \leq 700 \text{ nm}$) parts of the spectrum.

2.2. Model A

In model A (Fig. 2A), the partially linearly polarized second component with degree of polarization $p_{sc}(\lambda)$ was the sunlight undergoing first-order Rayleigh scattering



in the air layer between the ground observer and the foliage. By definition, the degree of linear polarization of downwelling light is the linearly polarized intensity divided by the total intensity:

$$p_A(\lambda, \theta) = \frac{ap_{sc}(\lambda)(I_{Sun}(\lambda, \theta)/\lambda^4)}{a(I_{Sun}(\lambda, \theta)/\lambda^4) + T(\lambda)I_{Sun}(\lambda, \theta)}, \quad (1)$$

where a is a weighting factor (control parameter) describing the ratio of the first (unpolarized) and second (polarized) components; $p_{sc}(\lambda)$ is the degree of linear polarization of scattered light from clear sky as given by Coulson (1988, p. 285) (Fig. 1A); $I_{Sun}(\lambda, \theta)$ is the spectrum of direct sunlight depending on the solar zenith angle θ (Fig. 1C); and $T(\lambda)$ is the spectrum of transmittance of cottonwood (*Populus deltoides*) leaves (Gates, 1980, p. 216) (Fig. 1D). The linearly polarized intensity is then

$$PI_A(\lambda, \theta) = p_A(\lambda, \theta) \left[a \frac{I_{Sun}(\lambda, \theta)}{\lambda^4} + T(\lambda)I_{Sun}(\lambda, \theta) \right] \\ = ap_{sc}(\lambda) \frac{I_{Sun}(\lambda, \theta)}{\lambda^4}. \quad (2)$$

In order for the usage of control parameter a to be consistent for all three models and for all illumination situations, a normalization was applied, which guaranteed that the two (unpolarized and polarized) components of the total intensity had equal contributions within our working wavelength range (between 300 and 700 nm) for $a = 1$. Thus, for model A, we performed the following normalization (on the left side polarized, on the right side unpolarized component of the total intensity):

$$\int_{300 \text{ nm}}^{700 \text{ nm}} \frac{I_{Sun}(\lambda, \theta)}{\lambda^4} d\lambda = \int_{300 \text{ nm}}^{700 \text{ nm}} T(\lambda)I_{Sun}(\lambda, \theta) d\lambda. \quad (3)$$

2.3. Model B

In model B (Fig. 2B), the partially linearly polarized second component was the light reflected from the epidermis (outer surface) of leaves, the degree of linear polarization δ of which was practically independent of the wavelength λ . Then, the degree of linear polarization and the linearly polarized intensity of downwelling

←
Fig. 2. Schematic representation of the two downwelling components of light reaching a cockchafer under a canopy in the case of the three investigated atmospheric optical models. In all three models the first component, called canopylight, is the unpolarized green light transmitted through the canopy. The second component is the partially linearly polarized sunlight (A) scattered in the air layer between the canopy and the cockchafer, (B) reflected from the leaf epidermis, or (C) reflected by both the leaf tissue and epidermis.

light were:

$$p_B(\lambda, \theta) = \frac{a\delta I_{Sun}(\lambda, \theta)}{aI_{Sun}(\lambda, \theta) + T(\lambda)I_{Sun}(\lambda, \theta)}, \quad (4)$$

and

$$PI_B(\lambda, \theta) = a\delta I_{Sun}(\lambda, \theta), \quad (5)$$

where δ was constant. The necessary normalization (when the unpolarized and polarized components of the total intensity have equal contributions for $a = 1$) was

$$\int_{300 \text{ nm}}^{700 \text{ nm}} I_{Sun}(\lambda, \theta) d\lambda = \int_{300 \text{ nm}}^{700 \text{ nm}} T(\lambda)I_{Sun}(\lambda, \theta) d\lambda. \quad (6)$$

2.4. Model C

In model C (Fig. 2C), the partially linearly polarized second component was the combination of the epidermis-reflected light and the light returned by the leaf tissue below the epidermis (where the light transmitted through the epidermis underwent diffuse scattering and then left the leaf tissue by refraction at the epidermis). For this model the degree of linear polarization of downwelling light was

$$p_C(\lambda, \theta) = \frac{ap_{leaf}(\lambda)R(\lambda)I_{Sun}(\lambda, \theta)}{aR(\lambda)I_{Sun}(\lambda, \theta) + T(\lambda)I_{Sun}(\lambda, \theta)}, \quad (7)$$

where $R(\lambda)$ was the spectrum of reflectance of cottonwood (*Populus deltoides*) leaves (Gates, 1980, p. 216) (Fig. 1D) and the function

$$p_{leaf}(\lambda) = K - Le^{-\frac{\ln 2(\lambda - \lambda_{min})^2}{\sigma^2}} \quad (8)$$

represented an approximation for the degree of linear polarization of the leaf-reflected component, which is shown in Fig. 1E for $K = 0.8$, $\lambda_{min} = 550 \text{ nm}$, $\sigma = 50 \text{ nm}$, and $L = 0.2, 0.4, 0.6$. According to the rule of Umow (1905), p_{leaf} is low in those spectral regions, where the leaf-reflected light is intense, and vice versa. In order to comply with this rule, the wavelength λ_{min} , where $p_{leaf}(\lambda)$ was minimal, was approximately set to the wavelength where $R(\lambda)$ was maximal. Thus, the linearly polarized intensity was

$$PI_C(\lambda, \theta) = ap_{leaf}(\lambda)R(\lambda)I_{Sun}(\lambda, \theta). \quad (9)$$

Again, we applied the necessary normalization:

$$\int_{300 \text{ nm}}^{700 \text{ nm}} R(\lambda)I_{Sun}(\lambda, \theta) d\lambda = \int_{300 \text{ nm}}^{700 \text{ nm}} T(\lambda)I_{Sun}(\lambda, \theta) d\lambda. \quad (10)$$

2.5. Calculation of quantum catch and quantum catch difference of DRA receptors under canopies illuminated by sunlight versus wavelength and solar zenith angle

As a receptor-physiological approach, we investigated the quantum catch Q and the quantum catch difference $\Delta \log Q$ of DRA photoreceptors with orthogonal microvilli. The photoreceptors were stimulated by downwelling light under canopies as calculated by the above three atmospheric optical models. Our aim was to estimate the spectral range in which a monochromatic DRA crossed-analyser detecting the polarization of downwelling light under canopies would function optimally. According to Horváth et al. (2002), if the E-vector of partially linearly polarized light is parallel (par) or perpendicular (perp) to the microvilli of a DRA photoreceptor, then the amount Q of light absorbed by the receptor (the quantum catch) is

$$Q_{par}(\lambda_{max}) = c \int A(\lambda, \lambda_{max})I(\lambda) \times [PS + 1 + (PS - 1)p(\lambda)] d\lambda, \quad (11)$$

$$Q_{perp}(\lambda_{max}) = c \int A(\lambda, \lambda_{max})I(\lambda) \times [PS + 1 - (PS - 1)p(\lambda)] d\lambda, \quad (12)$$

where c is a constant, and

$$A(\lambda, \lambda_{max}) = A_0 e^{-\frac{\ln 2(\lambda - \lambda_{max})^2}{\sigma^2}} \quad (13)$$

is the absorption spectrum of the receptor with $A_0 = 1$, and $\sigma = 50 \text{ nm}$ corresponding to that of *M. melolontha* (Labhart et al., 1992) (Fig. 1F); $I(\lambda)$ and $p(\lambda)$ are the intensity and the degree of linear polarization of light; PS is the polarization sensitivity ratio describing how a receptor absorbs PS -times more light when the E-vector of totally linearly polarized light is parallel to the microvilli, as opposed to perpendicular. In (13) A_0 is the maximum at $\lambda = \lambda_{max}$ and σ is the bandwidth of the receptor's absorption spectrum (in Fig. 1F the meaning of σ is explained visually by a horizontal vector). There are several different templates/nomograms for the description of the spectral absorption spectra or the spectral sensitivity functions of photoreceptors (e.g. Gouras, 1991). However, the majority of these templates share the common robust feature that their shape can be well approximated by a Gaussian function, which was also our approximation for the absorption spectrum of the photoreceptors in this paper. We note that our results were not sensitive to the choice of a particular template.

The E-vector contrast sensitivity of crossed-analysers in the DRA depends on the quantum catch difference

$$\Delta \log Q(\lambda_{max}) = \log Q_{par}(\lambda_{max}) - \log Q_{perp}(\lambda_{max}). \quad (14)$$

The greater the quantum catch difference $\Delta \log Q(\lambda_{max})$, the better the detection of polarization. Thus, maximizing $\Delta \log Q(\lambda_{max})$ is optimal for DRA receptors. We computed $\Delta \log Q(\lambda_{max})$ for wavelengths between 300 and 700 nm. We chose 700 nm as the upper wavelength limit in order to get a broader picture about how well different spectral ranges would suit the task of perceiving the polarization of downwelling light under canopies during sunset. This upper limit allowed us to compare the characteristics of $p(\lambda)$, $PI(\lambda)$, $\Delta \log Q(\lambda_{max})$, $\log Q_{par}(\lambda_{max})$ in the UV, blue, green and red parts of the spectrum.

We also calculated the logarithm of $Q_{par}(\lambda_{max})$ and $Q_{perp}(\lambda_{max})$, in order to provide another clue for the estimation of the optimal spectral range for detection of polarization of downwelling light under canopies. Because we obtained very similar results for $Q_{par}(\lambda_{max})$ and $Q_{perp}(\lambda_{max})$ here we only present results for $Q_{par}(\lambda_{max})$ [we note that $Q_{perp}(\lambda_{max})$ was never larger than $Q_{par}(\lambda_{max})$, because $PS + 1 - (PS - 1)p(\lambda) \leq PS + 1 + (PS - 1)p(\lambda)$].

3. Results

Fig. 3A shows the degree of linear polarization $p(\lambda)$ of downwelling light under a canopy calculated from atmospheric optical model A for values of 0.01, 0.05, 0.1, 0.2, 0.5, 1, 2, 5, 10, 100, and 1000 of the control parameter a and for solar zenith angle $\theta = 90^\circ$ (sunset). In model A, raising a means increasing the proportion of the partially linearly polarized sunlight scattered underneath the canopy (Fig. 2A). The degree of linear polarization $p(\lambda)$ has two major local maxima: $p_{short}(\lambda_{short})$ in the short-wavelength range (UV and blue, $360 \text{ nm} < \lambda_{short} < 470 \text{ nm}$), and $p_{long}(\lambda_{long})$ in the long-wavelength range (red, $\lambda_{long} \approx 675 \text{ nm}$). As a increases, both p_{short} and p_{long} increase, the difference $p_{short} - p_{long}$ decreases, λ_{short} shifts towards longer wavelengths, and λ_{long} does not change significantly. When λ is approximately 550 nm (green), $p(\lambda)$ reaches its major local minimum, which increases with a . Qualitatively similar results were obtained for all other solar zenith angles. In the family of curves $p(\lambda)$, the upper limit $p_{sc}(\lambda)$ is approached as a nears infinity. This case represents the absence of the unpolarized component (green canopy-light transmitted through the foliage). At a given value of a , $p(\lambda)$ uniformly shifts towards this upper limit as θ increases. Qualitatively similar results were obtained for model B (Fig. 3B) independently of δ , and for model C (Fig. 3C) independently of K and L . The only differences were that for models B and C, the short-wavelength maximum is at or under 300 nm, and that for model C there is a more pronounced fall in $p(\lambda)$ around 550 nm due to the characteristics of $p_{leaf}(\lambda)$ having its minimum at this wavelength. Nevertheless, considering the max-

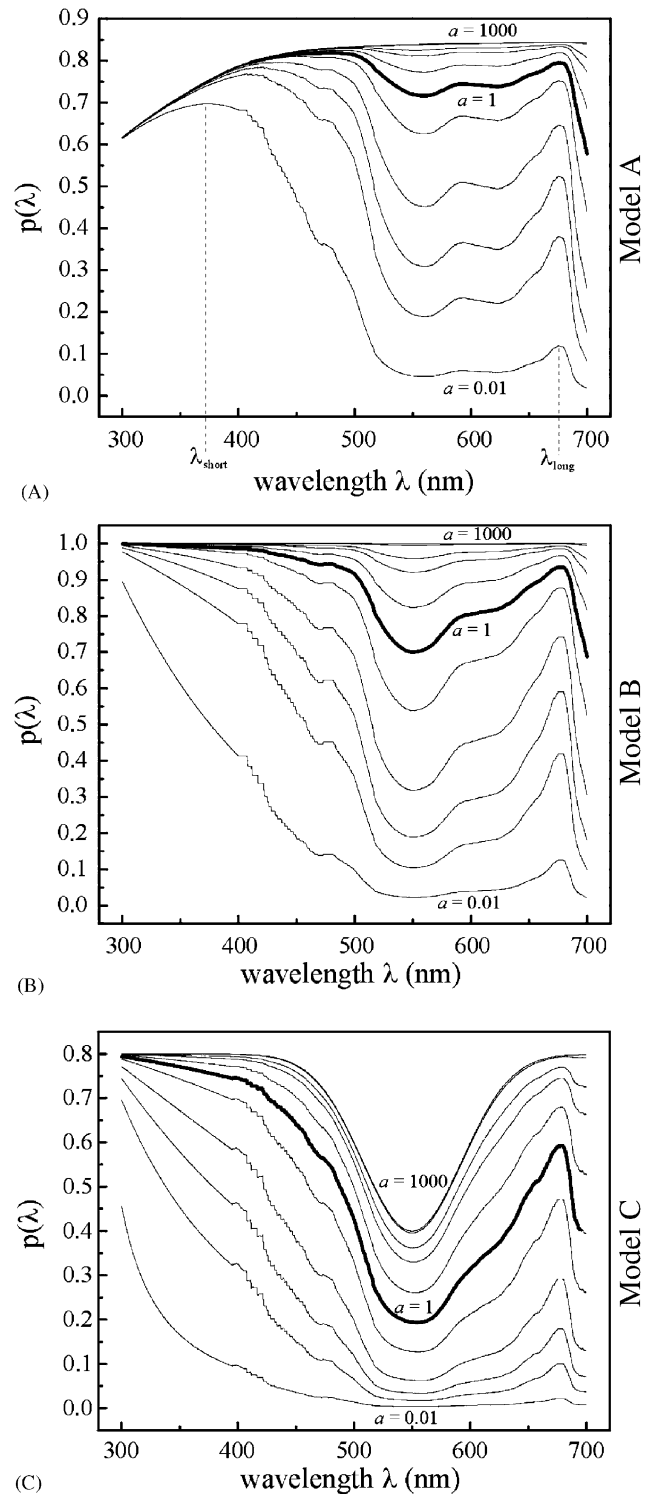


Fig. 3. Degree of linear polarization $p(\lambda, a)$ of downwelling light under a canopy calculated from atmospheric optical models A (A), B (B, with $\delta = 1$), and C (C, with $L = 0.4$) for $a = 0.01, 0.05, 0.1, 0.2, 0.5, 1, 2, 5, 10, 100,$ and 1000 (bottom to top), at solar zenith angle $\theta = 90^\circ$. Qualitatively similar results were obtained for other $\theta, L,$ and δ . Increasing value of the control parameter a means increasing the proportion of partially linearly polarized sunlight scattered underneath the canopy (model A), reflected from the leaf epidermis (model B), or reflected by both the leaf tissue and epidermis (model C).

imization of $p(\lambda)$, in all three models the UV-blue and red are the first and second most advantageous spectral ranges, respectively, and green is the most disadvantageous part of the spectrum for detection of polarization of downwelling light under canopies, independently of solar zenith angle.

In the retina of *M. melolontha*, the sensitivity of DRA receptors is maximal at $\lambda = 520$ nm. Although not minimal, $p(\lambda)$ is still very much lower at this wavelength than in the UV-blue and red portions of the spectrum, except when a is extremely high. Therefore, we conclude that the green sensitivity of DRA receptors in cockchafers cannot be explained by means of an adaptation to the wavelengths of maximal values of degree of polarization (p_{short} and p_{long}) of downwelling light under canopies. One explanation could be that high-enough p of downwelling light is only one prerequisite of polarization vision under canopies. In addition, the intensity I also needs to be sufficiently high for detection of polarization, especially during sunset, when I considerably and rapidly decreases with increasing solar zenith angle. To decide whether p and I are simultaneously high enough at any given wavelength, the linearly polarized intensity $PI(\lambda) = p(\lambda)I(\lambda)$ should be investigated.

Fig. 4A shows $PI(\lambda)/a$ of downwelling light under a canopy, calculated from atmospheric optical model A for solar zenith angles $\theta = 30^\circ, 80^\circ, 85^\circ, 90^\circ$. As θ increases from 0 to 90° , the wavelength where PI is maximal shifts from violet-blue toward the red spectral range. Hence, prior to sunset, PI is maximal in the green, and at sunset PI is sufficiently high in the green, while at the same time being very much higher than in the short (blue, violet, UV) wavelength range. Qualitatively similar results were obtained for model B (Fig. 4B), independently of δ , as well as for model C (Fig. 4C) independently of K and L . Directly before and at sunset, PI is usually highest in the red, it is always relatively high in the green, and particularly low at shorter wavelengths. Based on these findings we conclude that the spectral sensitivity of DRA receptors in cockchafers is tuned to the maximal or sufficiently high polarized intensity PI of downwelling light in the green part of the spectrum under canopies during sunset.

Figs. 5A and B show the difference $\Delta \log Q(\lambda_{max})$ in the logarithm of the quantum catches of our two polarization-sensitive model receptors with orthogonal microvilli calculated from atmospheric optical model A for $a = 0.01, 0.05, 0.1, 0.2, 0.5, 1, 2, 5, 10, 100$, and 1000 and for solar zenith angles $\theta = 30^\circ$, and 90° . If $a < 5-10$, as a increases the wavelength where $\Delta \log Q(\lambda_{max})$ is maximal shifts from the UV (< 400 nm) towards the blue (480 nm) for $\theta = 30^\circ$ (Fig. 5A), but remains in the UV for $\theta = 90^\circ$ (Fig. 5B). The quantity $\Delta \log Q(\lambda_{max})$ has a plateau (or a secondary local maximum) ranging from approximately 570–650 nm for $\theta = 30^\circ$ (Fig. 5A)

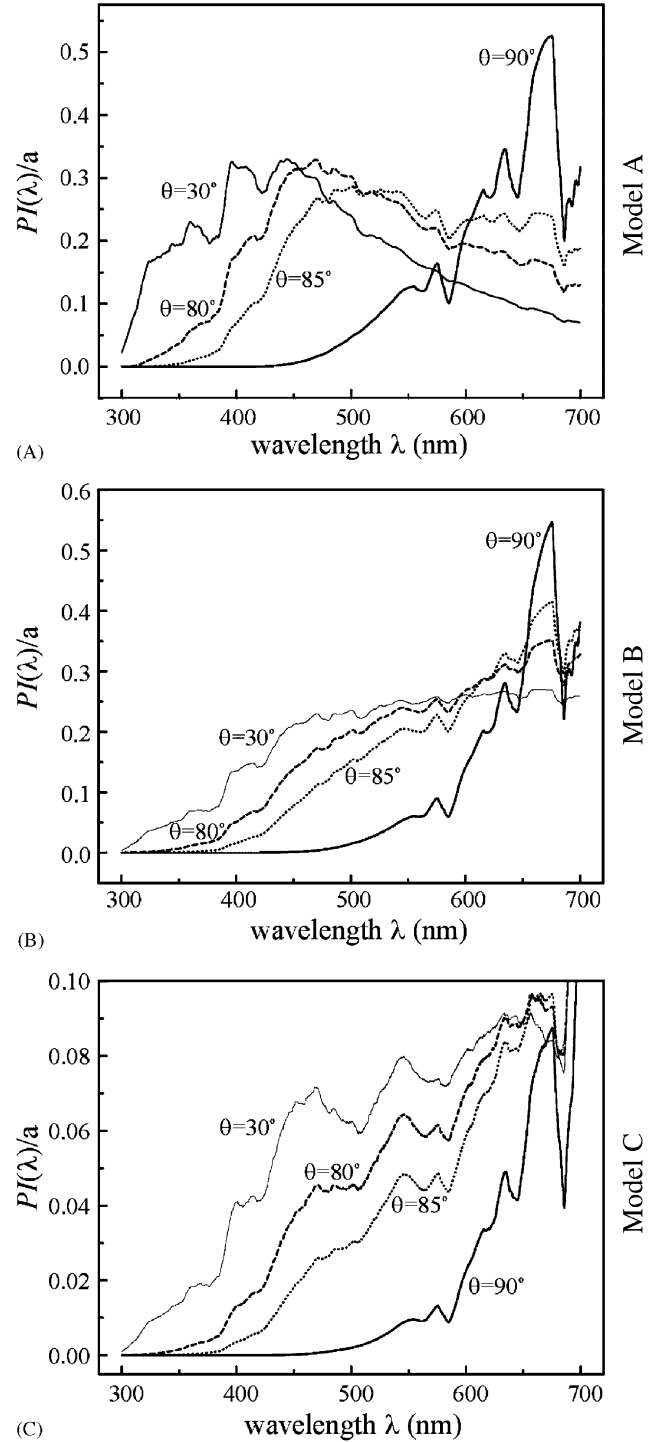
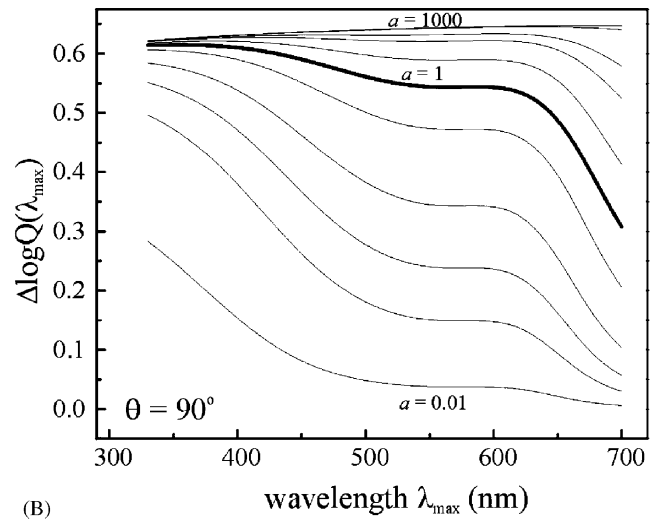
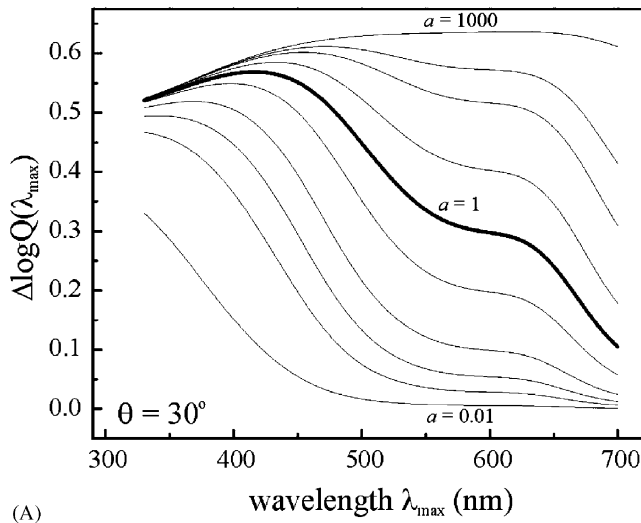


Fig. 4. $PI(\lambda)/a$, where $PI(\lambda)$ is the linearly polarized intensity of downwelling light under a canopy, and a is the control parameter, calculated from atmospheric optical models A (A), B (B, with $\delta = 1$), and C (C, with $L = 0.4$) for solar zenith angles $\theta = 30^\circ, 80^\circ, 85^\circ$, and 90° . Qualitatively similar results were obtained for other θ, L , and δ .

and from 520 to 620 nm for $\theta = 90^\circ$ (Fig. 5B). The difference between maximum and plateau values of $\Delta \log Q(\lambda_{max})$ diminishes with increasing a . At a given value of a , $\Delta \log Q(\lambda_{max})$ increases with increasing θ .

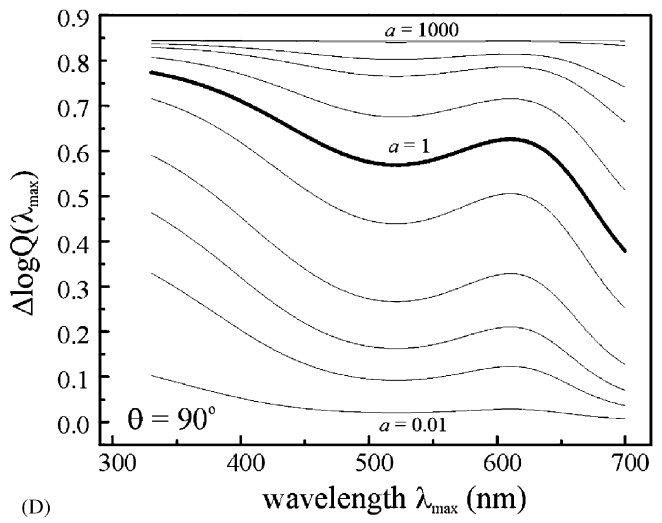
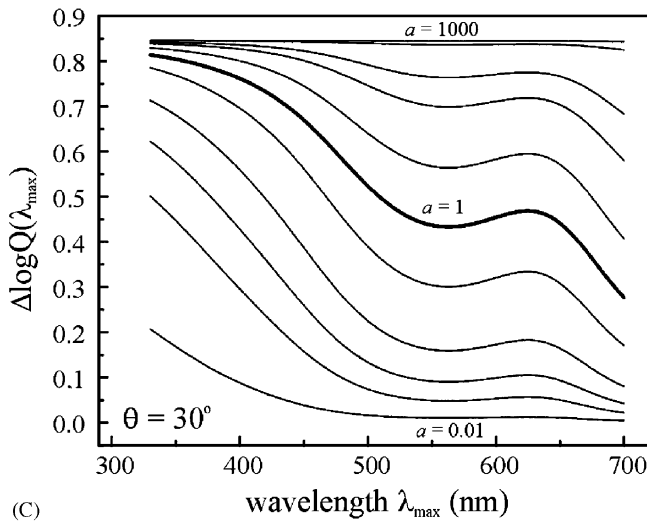
Model A



(A)

(B)

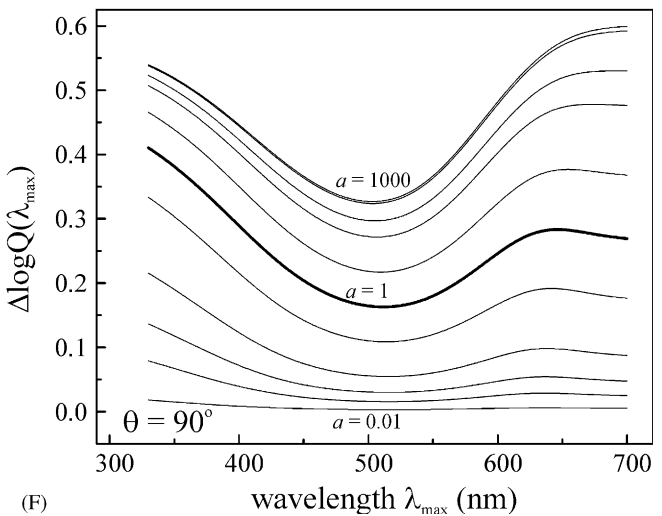
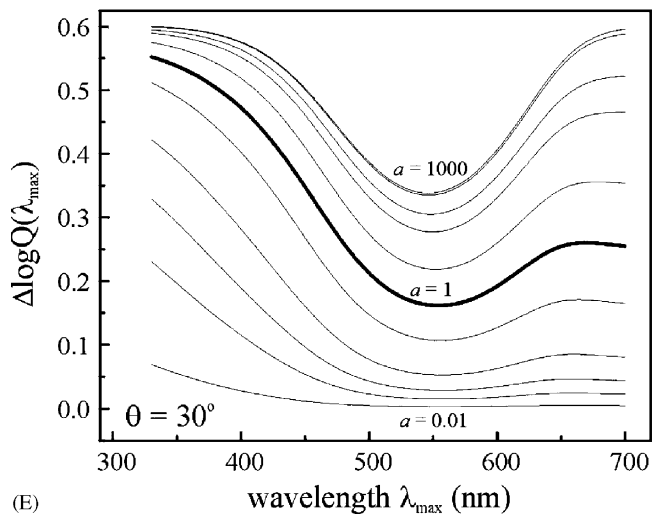
Model B



(C)

(D)

Model C



(E)

(F)

Fig. 5. Quantum catch difference $\Delta \log Q(\lambda_{\max}, a)$ of our polarization-sensitive model receptors with orthogonal microvilli calculated from atmospheric optical models A (A, B), B (C, D; with $\delta = 1$), and C (E, F; with $L = 0.4$) for $a = 0.01, 0.05, 0.1, 0.2, 0.5, 1, 2, 5, 10, 100$, and 1000 (bottom to top), at solar zenith angles $\theta = 30^\circ$ (A, C, E) and $\theta = 90^\circ$ (B, D, F). Qualitatively similar results were obtained for other θ, L , and δ .

Considering the maximization of $\Delta \log Q(\lambda_{max})$ according to model A, we found that for $a < 5$ –10 the shorter the wavelength λ_{max} , the more efficient the detection of polarization of downwelling light under canopies, independently of solar zenith angle. If $a > 5$ –10, then $\Delta \log Q(\lambda_{max})$ is practically constant for $\lambda_{max} > 500$ nm at $\theta = 30^\circ$ and for $\lambda_{max} > 400$ nm at $\theta = 90^\circ$, while being approximately as high as in the UV.

From these relationships we conclude that considering the maximization of $\Delta \log Q(\lambda_{max})$, green receptors in the DRA of cockchafers are less advantageous than blue or UV receptors for $a < 5$ –10, but that the opposite is true for $a > 5$ –10, independently of solar zenith angle. Thus, the green sensitivity of DRA receptors in *M. melolontha* could serve the maximization of the quantum catch difference $\Delta \log Q(\lambda_{max})$, if the proportion a of the partially linearly polarized sunlight scattered underneath the canopy is sufficiently high. Otherwise, green sensitivity, though less advantageous, can still be satisfactory considering that $\Delta \log Q(\lambda_{max})$ is not much lower around $\lambda_{max} = 520$ nm than in the short (blue, violet, or UV) wavelength range. This conclusion does not hold true when the partially linearly polarized component of the downwelling light under canopy has less contribution than the unpolarized component ($a < 1$), as would be the case in deep continuous vegetation canopies. So there may be some habitat selection by cockchafers to prefer thin enough canopy for this to work. In model B, $\Delta \log Q(\lambda_{max})$ always has a secondary local maximum at wavelengths where the plateau of $\Delta \log Q(\lambda_{max})$ occurs in model A (Fig. 5C,D). Furthermore, considering the maximization of $\Delta \log Q(\lambda_{max})$ in model B, apart from very high values of a (> 100) when there is no wavelength preference, green-sensitive DRA receptors are less advantageous than blue- or UV-sensitive ones, independently of θ and δ (Fig. 5C,D). Considering the maximization of $\Delta \log Q(\lambda_{max})$ in model C, apart from very small values of a (< 0.01 – 0.05) when there is no wavelength preference, green-sensitive DRA receptors are less advantageous than blue- or UV-sensitive ones, independently of θ , K and L (Fig. 5E,F). However, in the UV and blue part of the spectrum, the quantum catch $Q(\lambda_{max})$ is much lower than in the green at large solar zenith angles (Fig. 6). Consequently, the use of green-sensitive DRA receptors can be interpreted as an optimal compromise between maximization of $\Delta \log Q(\lambda_{max})$ and $Q(\lambda_{max})$.

Figs. 6A and B show the logarithm of the quantum catch $Q_{par}(\lambda_{max})$ of our polarization-sensitive model

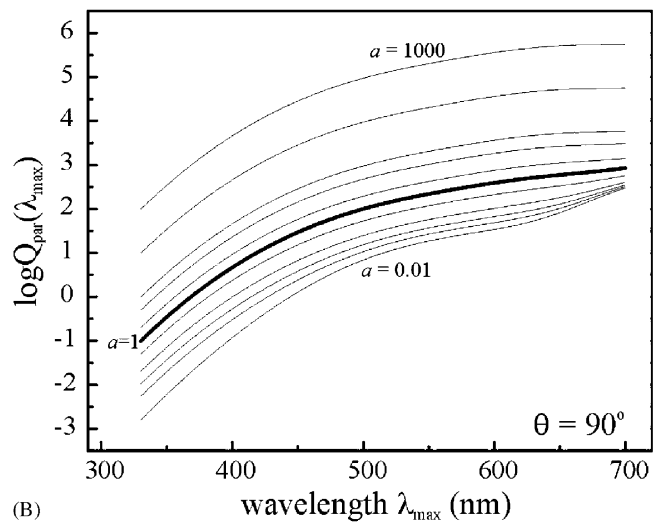
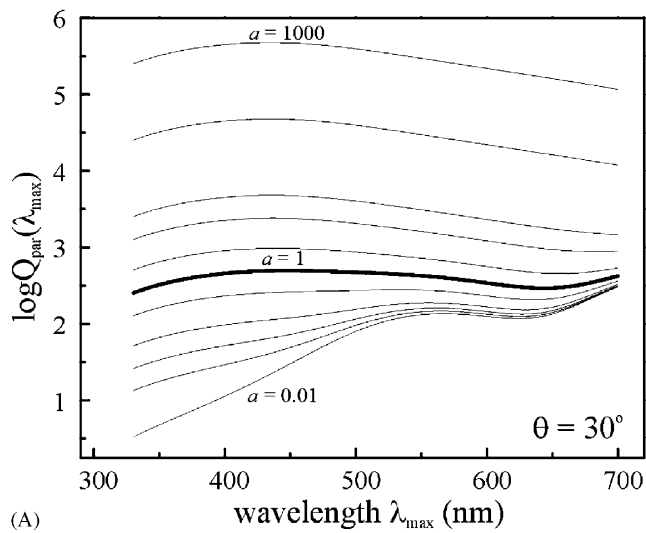
receptor with microvilli parallel to the direction of polarization of downwelling light, calculated from atmospheric optical model A for $a = 0.01, 0.05, 0.1, 0.2, 0.5, 1, 2, 5, 10, 100, \text{ and } 1000$ and for solar zenith angles $\theta = 30^\circ$, and 90° . If $\theta > 80^\circ$, $Q_{par}(\lambda_{max})$ monotonically increases with increasing λ_{max} , independently of a . In this case, red-sensitive DRA receptors absorb much more downwelling light than green-sensitive receptors, which in turn absorb much more light than blue- or UV-sensitive ones. In cases where $\theta < 80^\circ$, the situation is more complex (Fig. 6A). If $a > 2$, $Q_{par}(\lambda_{max})$ is maximal at approximately 420 nm, and blue-sensitive DRA receptors absorb the most amount of light. If $0.5 < a < 2$, $Q_{par}(\lambda_{max})$ is basically constant for $\lambda < 700$ nm; thus, there is no preferred wavelength. If $a < 0.5$, $Q_{par}(\lambda_{max})$ monotonically increases with λ_{max} , therefore DRA receptors sensitive to longer wavelengths are favoured. For all three models, our basic finding is that at small solar zenith angles, the change in the quantum catch from the UV towards the red is usually smaller than one order of magnitude, except when a is extremely low. On the other hand, quantum catch changes can be as high as five orders of magnitude during sunset, and $Q_{par}(\lambda_{max})$ always monotonically increases with λ_{max} , regardless of a . Furthermore, the difference in quantum catch between the green and UV is two to three orders of magnitude at dusk. These establishments hold for any values of δ in model B, and of K and L in model C. Based upon these findings, we conclude that green sensitivity of DRA receptors in cockchafers serves to maximize the quantum catch under canopies during sunset, because only UV, blue, and green receptor types are available.

4. Discussion

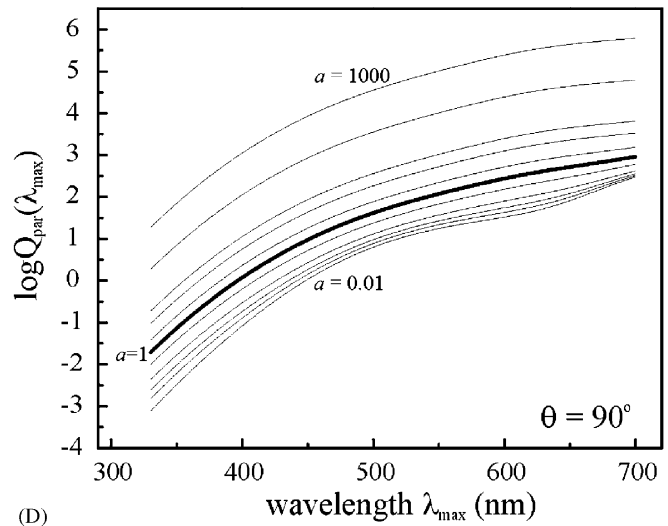
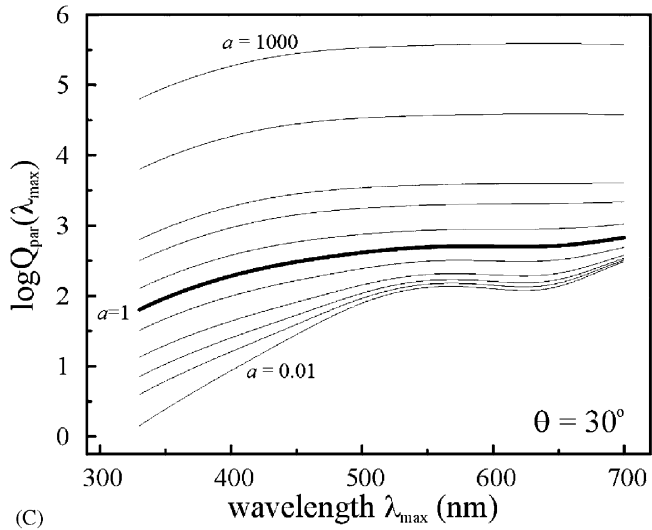
To the best of our knowledge, our work is the first that deals with the explanation of the green sensitivity of polarization vision in cockchafers. Here we showed that there could be atmospheric optical, receptor physiological, and behavioural reasons for this green sensitivity. Our results proved that it would be worth measuring polarization patterns under tree canopies as a function of solar zenith angle in different parts of the spectrum, in order to study further this phenomenon. In the future this task can efficiently be performed by 180° field-of-view imaging polarimetry (Gál et al., 2001; Horváth et al., 2002; Horváth and Varjú, 2003).

Fig. 6. Logarithm of the quantum catch $Q_{par}(\lambda_{max}, a)$ of our polarization-sensitive model receptor with microvilli parallel to the E-vector of downwelling light calculated from atmospheric optical models A (A, B), B (C, D; with $\delta = 1$), and C (E, F; with $L = 0.4$) for $a = 0.01, 0.05, 0.1, 0.2, 0.5, 1, 2, 5, 10, 100, \text{ and } 1000$ (bottom to top) at solar zenith angles $\theta = 30^\circ$ (A, C, E) and $\theta = 90^\circ$ (B, D, F). Qualitatively similar results were obtained for other θ , L , and δ , as well as for $Q_{perp}(\lambda_{max}, a)$.

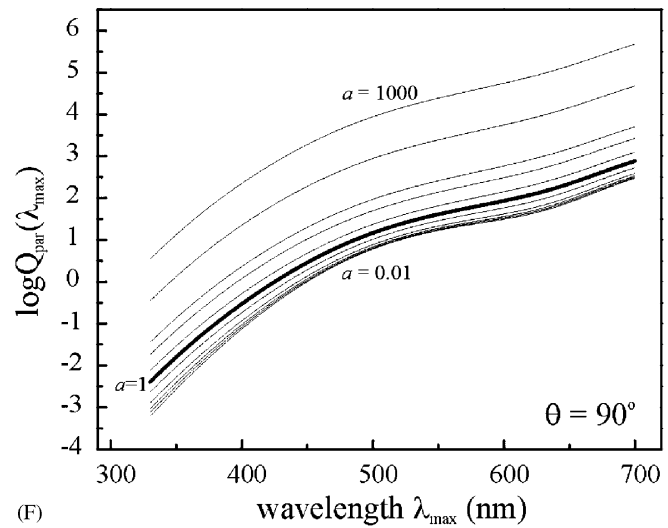
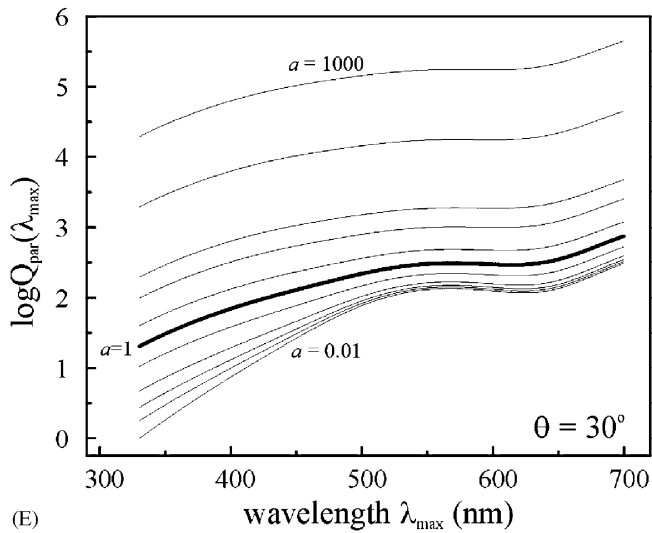
Model A



Model B



Model C



Adult European cockchafers (alias maybeetles, *M. melolontha* Linnaeus, Coleoptera: Scarabaeidae), are serious pests to human agriculture and horticulture, because they feed on forest and fruit tree leaves. Egg deposition and larval development take place in the soil of open fields and orchards, and adult beetles gather at the edges of relatively open forests to feed and mate (Schneider, 1952). In April and May after hibernation, adult cockchafers leave their overwintering sites. Flying singly, particularly at dusk, they migrate towards feeding sites positioned at forest edges or on isolated trees. This flight is called the “pre-feeding flight”. The flight at sunset is called the “swarming flight”, as cockchafers hover around treetops and mate on host trees (Schneider, 1952). Hovering cockchafers are almost exclusively males, scanning the host trees for receptive females who remain feeding on the host trees. Warm and dry weather favours swarming, whereas rainy and cool days inhibit swarming. Both males and females mate several times, and mating can last for several hours (Krell, 1996). Males orient themselves toward the “green leaf volatiles” emitted by leaves damaged by eating females (Imrei and Tóth, 2002). Males also use a female-derived sex pheromone to find mates and are able to discriminate between leaf damage caused by feeding females and non-specific leaf damage (Reinecke et al., 2002). After 10–15 days of feeding, females have acquired sexual maturity and make an “egg-laying flight” toward open fields and meadows in the opposite direction of the pre-feeding flight, ovipositing in the soil upon landing. While many egg-laying females die upon ovipositing, about a third return to feed and lay for a second time, with some even laying for a third time (Krell, 1996). After 4–6 weeks of embryonic development, larvae hatch and continue to develop in the soil for 3–4 years (Schneider, 1952).

From the above it is clear that during their lifetime cockchafers fly in two significantly different optical environments during sunset: (i) under clear or cloudy skies during their pre-feeding and egg-laying flights, and (ii) under canopies illuminated by the setting sun during their swarming flights. Although *M. melolontha* is one of the best known insect species in central Europe, hardly anything is known about how its orientation is governed by polarization vision, nor how it orients itself under both sky and tree canopy. Nevertheless, cockchafers obviously use their polarization-sensitive DRA receptors for orientation in both types of optical environment.

Cockchafers swarming at dusk under trees at forest borders are confronted with a light environment that tends to be patchy and has been studied in some detail regarding the spectral composition of light (Endler, 1993). According to Endler (1993), the structure of forests leads to four major light habitats when the sun is not blocked by clouds: forest shade, woodland shade,

small gaps, and large gaps. These are characterized by yellow-green, blue-gray, reddish, and white ambient light spectra, respectively. An additional light environment is associated with low solar elevation angles near dawn and dusk, which is purplish. Apart from a preliminary study by Shashar et al. (1998), the polarizational characteristics of the light environment in forests and at forest edges have not been thoroughly measured. This is an important task of future research motivated by our results presented here.

In this work, we investigated whether the green-sensitive DRA receptors in *M. melolontha* could serve for orientation based on linear polarization of downwelling light under canopies. Our investigations were based upon an atmospheric optical and receptor-physiological approach. Considering atmospheric optics, the primary condition for successful detection of light polarization is that linearly polarized intensity must be over the stimulus threshold of photoreceptors. Only if this prerequisite is fulfilled, can the degree of linear polarization p be considered. Analogously, according to the receptor-physiological approach, receptors need to catch enough light quanta to be able to detect polarization by comparing the quantum catches of two receptor types with orthogonal microvilli (crossed-analyser in the DRA). Thus, the optimal strategy for achieving a successful and efficient orientation by means of linear polarization of downwelling light is to select a spectral range of sensitivity for the receptors, where both $PI(\lambda)$ and $p(\lambda)$ (in the atmospheric optical term), and both $\Delta \log Q(\lambda_{max})$ and $\log Q(\lambda_{max})$ (in the receptor-physiological term) are simultaneously maximal or at least sufficiently high. When the spectral ranges, where $PI(\lambda)$, $p(\lambda)$, $\Delta \log Q(\lambda_{max})$, and $\log Q(\lambda_{max})$ are maximal or sufficiently high, greatly overlap, the optimal spectral range for detection of polarization is the overlapping portion of the spectrum. This is the case when detecting skylight polarization under clear sky with high solar elevation, but not when detecting polarization of downwelling light under canopies during sunset.

Based upon our computations, we conclude that the green-sensitive DRA receptors in *M. melolontha* are not tuned to the maximal degree of linear polarization $p(\lambda)$ of downwelling light under canopies. Under these circumstances $p(\lambda)$ is minimal in the green, maximal in the UV, and it is still considerably greater in the blue and red than in the green for all solar zenith angles (Fig. 3). However, this is not a serious problem for cockchafers for two reasons. First, $p(\lambda)$ increases as the sun approaches the horizon and cockchafers begin their activity. Second, unless the proportion a of the partially linearly polarized sunlight scattered underneath the canopy (model A), or reflected from the leaf epidermis (model B), or reflected by both the leaf tissue and epidermis (model C) is well below 1, there is only a

moderate fall in $p(\lambda)$ from shorter wavelengths (UV, violet, blue) towards the green. Thus, in the green portion of the spectrum $p(\lambda)$ of downwelling light under canopies remains sufficiently high for polarization vision, especially near sunset. We note here that the prerequisite for polarization vision in honeybees and field crickets is that $p > 0.10$ and $p > 0.05$, respectively (Horváth and Varjú, 2003). Under canopies during sunset, a more serious problem is the rapidly decreasing intensity $I(\lambda)$ of downwelling light, because $I(\lambda)$ determines the polarized intensity $PI(\lambda)$. The UV and blue portion of PI , however, is significantly lower than the green one during sunset (Fig. 4). Consequently, the spectral sensitivity of DRA receptors in *M. melolontha* is tuned to the maximal or sufficiently high green component of PI of downwelling light under canopies at sunset. In the green spectral range p is also sufficiently high for polarization vision.

A similar conclusion can be drawn by analyzing the quantum catch difference $\Delta \log Q(\lambda)$ and the quantum catch $Q(\lambda)$ (Figs. 5 and 6): $\Delta \log Q(\lambda)$, which is the measure of the efficiency of the detection of polarization, is generally higher in the UV and blue than in the green (Fig. 5). Thus, considering only the maximization of $\Delta \log Q(\lambda)$, green-sensitive DRA receptors would be less advantageous than blue- or UV-sensitive ones under canopies. During sunset, however, $Q(\lambda)$ diminishes strongly with decreasing λ (Fig. 6), therefore the quantum catch of UV- and blue-sensitive DRA receptors would certainly be too small, and only green-sensitive receptors have large enough Q for the detection of polarization. Consequently, the use of green-sensitive DRA receptors in cockchafer is an optimal compromise between simultaneous maximization of $\Delta \log Q(\lambda)$ (Fig. 5) and $Q(\lambda)$ (Fig. 6).

During the pre-feeding and egg-laying cockchafer flights at dusk, the optimal wavelength range of DRA receptors would be the blue part of the spectrum. This explains why DRA receptors in dusk-active crickets orienting under twilight skies are blue sensitive (Labhart et al., 1984; Herzmann and Labhart, 1989; Zufall et al., 1989; Horváth and Varjú, 2003; Barta and Horváth, 2004). For the cockchafer swarming flight under canopies at sunset, however, the optimal spectral range for DRA receptors is the long-wavelength segment of the spectrum. Therefore, red-sensitive DRA receptors would be the most advantageous for this task, because the degree of linear polarization, the linearly polarized intensity, the quantum catch, and the quantum catch difference are all simultaneously maximal or sufficiently high in the red spectral range. However, red receptors generally do not occur in beetles (Briscoe and Chittka, 2001). Since the DRA receptors in *M. melolontha* are green sensitive, they may serve the swarming flight best (for which longer wavelengths are optimal), rather than the pre-feeding and egg-laying flights (for which shorter

wavelengths are optimal). The pre-feeding and egg-laying flights occur prior to sunset when the intensity of skylight in the green is still relatively high; thus, green-sensitive DRA receptors could still serve orientation by means of skylight polarization.

All of our atmospheric optical models assume that the canopy is illuminated by direct light from the setting sun. This condition would not be satisfied were the setting sun occluded by clouds on overcast days. However, on cloudy days cockchafers generally do not perform swarming flights. One explanation could be that under such conditions the degree of linear polarization, and/or the polarized intensity, and/or the quantum catch, and/or the quantum catch difference, may be too small for the detection of polarization. On the other hand, after sunset (when the sun is below the horizon) there is no direct sunlight and the diffuse blue skylight dominates. Then there is a reduction of light intensity with a maximum reduction around 602 nm due to ozone, but there is still enough light at about 550 nm (Gates, 1980; Endler, 1993). Note, however, that our conclusions are valid prior to sunset when the sunlight illuminating the tree canopies and the air layer beneath them changes from predominantly green to yellow to orange and then to red as the solar elevation angle gradually decreases. Under these illumination conditions there is still enough downwelling linearly polarized green light that can serve for polarization vision in dusk-active cockchafers. In addition, if it is cloudy and the setting sun illuminates clouds on the dark side of the terminator (earth's shadow on the earth's surface), then these clouds re-radiate reddish light (Endler, 1993). This may profoundly alter the lighting conditions, but this makes no difference given that the cockchafers usually do not swarm.

In principle, we could develop a complex atmospheric optical model that would simultaneously treat the three different polarized components of light characterized separately by models A, B, and C. Each of our simple atmospheric models, however, leads to the same conclusion regarding the usefulness of green polarization sensitivity of DRA receptors in *M. melolontha*. This renders it unnecessary to implement a united model, which would introduce several free parameters and thus, would be hard to evaluate.

We also need to briefly discuss realistic values of the control parameter a (varying between 0.01 and 1000 in Figs. 3, 5, and 6) involved in all three atmospheric models. Parameter a gives the proportion of the partially linearly polarized sunlight (A) scattered underneath the canopy in model A, or (B) reflected from the leaf epidermis in model B, or (C) reflected by both the leaf tissue and epidermis in model C. Although there are no measurements available to determine the ratio of unpolarized and linearly polarized components of downwelling light under canopies, we argue that neither

component has an overwhelming contribution in the visual environment of cockchafers. First, very high a (> 10) would mean that the unpolarized canopylight is insignificant. This could be conceivable only if the canopy consisted of leaves so thick that there was no transmitted light, situations not typical in nature. Second, if the canopy were too dense the polarized component would also be highly absorbed, which would result in low a (< 0.1). Third, an extremely low a (< 0.01) would mean that virtually no direct sunlight could reach the air layer beneath the foliage, which could only be a realistic situation within forests. However, in such a case, the orientation by means of polarization would be impossible in any spectral range. Cockchafers do not live and orient inside dense forests, but prefer the forest edges, places where the effects we model are most likely to occur. Therefore, we conclude that in practice, non-extreme values of a (i.e. neither very much greater, nor very much smaller than 1) should be considered. We estimate that the typical range of parameter a in the optical environment of cockchafers is about $0.1 < a < 10$.

Barta and Horváth (2004) have shown that UV light is optimal for detection of polarization of downwelling light under tree canopies illuminated by daylight, when the sun is high above the horizon. Here, the same conclusion was corroborated for smaller ($\theta = 30\text{--}60^\circ$) solar zenith angles (Fig. 3). However, in this work we also showed that green light is optimal for detection of polarization of downwelling light under tree canopies illuminated by the setting sun. Our main result is that there is more polarized green light available under tree canopies during sunset, which may be the reason for the green sensitivity of the polarization channel in dusk-active cockchafers swarming under trees. Generally, there is more green light available in the forest than it is experienced by the naked eye. However, the problem of the spectral sensitivity of polarization vision in cockchafers is much more complex than simply reducing it to the intensity of available light. Here we showed that the linearly polarized intensity of downwelling light is the relevant parameter which determines the optimal spectral range for polarization vision under trees during sunset. Hence, it is not the light intensity, but the polarized intensity (which is the product of the total intensity and the degree of linear polarization) that constitutes a limiting factor for dusk-active cockchafers. If the intensity of green light were relatively high, but its polarization were not strong enough, the polarization vision of cockchafers could not function in the green during sunset.

Our atmospheric optical and receptor-physiological arguments are valid for downwelling light under canopies illuminated by the setting sun. However, they cannot explain green sensitivity of DRA receptors in the dusk- and night-active beetle *P. armaticeps* (Coleoptera: Tenebrionidae), which inhabits the Kalahari desert in

southern Africa (Heg and Rasa, 2004). This beetle has to orient under predominantly clear twilight skies. Considering the perception of skylight polarization under clear skies, there is no favoured wavelength because the degree of linear polarization is sufficiently high (much higher than the threshold of polarization sensitivity) at all wavelengths (Fig. 1A). Thus, the proportion of the celestial polarization pattern useful for orientation is sufficiently large at all wavelengths, both in the UV and visible parts of the spectrum (Horváth and Varjú, 2003; Barta and Horváth, 2004). As we mentioned in the introduction, crickets possess blue-sensitive DRA receptors, thereby avoid the very low intensity I of skylight in the UV at dusk, and utilize the maximal I (Figs. 1B, C) and the relatively high p (Fig. 1A) of skylight in the blue (Fig. 1A). The green-sensitive DRA receptors in *P. armaticeps* can also function efficiently enough at twilight, because they avoid the very low I in the UV at dusk, and utilize the relatively high I , and the maximal p of skylight in the green (Figs. 1A, B, C).

Finally, we would like to emphasize that beyond our atmospheric optical and receptor-physiological arguments, certainly other important biological and/or environmental factors may exist which determine the optimal wavelength range for the detection of polarization of downwelling light in cockchafers. Our paper, based upon the study of the spectral and polarizational characteristics of downwelling light under canopies illuminated by the setting sun is the first that explains why it might be evolutionarily advantageous for cockchafers to detect polarization in the green.

Acknowledgements

This work was supported by a 3-year István Széchenyi research fellowship from the Hungarian Ministry of Education and an equipment donation from the German Alexander von Humboldt Foundation received by Gábor Horváth. We thank Cynthia J. Archerd for proofreading an earlier version of the manuscript. We are grateful for the comments of Professor John A. Endler (Department of Ecology, Evolution and Marine Biology, University of California, Santa Barbara, USA) and two anonymous reviewers.

References

- Barducci, A., Castagnoli, F., Guzzi, D., Marcoianni, P., Pippi, I., Poggesi, M., 2004. Solar spectral irradiometer for validation of remotely sensed hyperspectral data. *Appl. Opt.* 43, 183–195.
- Barta, A., Horváth, G., 2004. Why is it advantageous for animals to detect celestial polarization in the ultraviolet? Skylight polarization under clouds and canopies is strongest in the UV. *J. Theor. Biol.* 226, 429–437.
- Berk, A., Bernstein, L.S., Robertson, D.C., 1983. MODTRAN: a moderate resolution model for LOWTRAN 7. Air Force Geophy-

- sical Laboratory Technical Report GL-TR-83-0187, Hanscom Air Force Base, MA 01731-5000.
- Bisch, S.M., 1999. Orientierungsleistungen des nachtaktiven Wüstenkäfers *Parastizopus armaticeps* Peringuey (Coleoptera: Tenebrionidae). Ph.D. Thesis, University Bonn, Germany.
- Brines, M.L., Gould, J.L., 1982. Skylight polarization patterns and animal orientation. *J. Exp. Biol.* 96, 69–91.
- Briscoe, A.D., Chittka, L., 2001. The evolution of color vision in insects. *Ann. Rev. Entomol.* 46, 471–510.
- Cebula, R.P., Thuillier, G.O., VanHoosier, M.E., Hilsenrath, E., Herse, M., Brueckner, G.E., Simon, P.C., 1996. Observations of the solar irradiance in the 200–350 nm interval during the ATLAS-1 mission: a comparison among three sets of measurements—SSBUV, SOLSPEC, and SUSIM. *Geophys. Res. Lett.* 23, 2289–2292.
- Chance, K.V., Spurr, R.J.D., 1997. Ring effect studies: Rayleigh scattering, including molecular parameters for rotational Raman scattering, and the Fraunhofer spectrum. *Appl. Opt.* 36, 5224–5230.
- COESA, 1976. US Standard Atmosphere. US Government Printing Office, Washington, DC.
- Coulson, K.L., 1988. Polarization and Intensity of Light in the Atmosphere. A Deepak Publishing, Hampton, Virginia, USA.
- Endler, J.A., 1993. The color of light in forests and its implications. *Ecol. Monogr.* 63, 1–27.
- Gál, J., Horváth, G., Meyer-Rochow, V.B., Wehner, R., 2001. Polarization patterns of the summer sky and its neutral points measured by full-sky imaging polarimetry in Finnish Lapland north of the Arctic Circle. *Proc. R. Soc. London A* 457, 1385–1399.
- Gates, D.M., 1980. *Biophysical Ecology*. Springer, Heidelberg, Berlin, New York.
- Gouras, P., 1991. The perception of colour. In: Cronly-Dillon, J.R. (Ed.), *Vision and Visual Dysfunction*, vol. 6. The Macmillan Press Ltd., London, UK.
- Halhore, R.N., Schwartz, E.S., Michalsky, J.J., Anderson, G.P., Ferrare, R.A., Holben, B.N., Brink, H.M.T., 1997. Comparison of model estimated and measured direct-normal solar irradiance. *J. Geophys. Res. D* 102, 29991–30002.
- Heg, D., Rasa, O.A.E., 2004. Effects of parental body condition and size on reproductive success in a tenebrionid beetle with biparental care. *Ecol. Entomol.* 29, 410–419.
- Herzmann, D., Labhart, T., 1989. Spectral sensitivity and absolute threshold of polarization vision in crickets: a behavioral study. *J. Comp. Physiol. A* 165, 315–319.
- Horváth, G., Varjú, D., 2003. *Polarized Light in Animal Vision—Polarization Patterns in Nature*. Springer, Heidelberg, Berlin, New York.
- Horváth, G., Barta, A., Gál, J., Suhai, B., Haiman, O., 2002. Ground-based full-sky imaging polarimetry of rapidly changing skies and its use for polarimetric cloud detection. *Appl. Opt.* 41, 543–559.
- Imrei, Z., Tóth, M., 2002. European common cockchafer (*Melolontha melolontha* L.): preliminary results of attraction to green leaf odours. *Acta Zool. Acad. Sci. Hung.* 48 (Suppl. 1), 151–155.
- Krell, F.T., 1996. The copulatory organs of the cockchafer, *Melolontha melolontha* (Insecta: Coleoptera: Scarabaeidae). A contribution to comparative and functional anatomy of ectodermal genitalia of the Coleoptera. *Stuttg. Beitr. Naturk. A* 537, 1–101.
- Kurucz, R.L., 1995. The solar irradiance by computation. In: Anderson, G.P., Picard, R.H., Chetwynd, J.H. (Eds.), *Proceedings of the 17th Annual Review Conference on Atmospheric Transmission Models*. Phillips Lab., Geophys. Dir., Bedford, MA 332pp.
- Labhart, T., Meyer, E.P., 1999. Detectors for polarized skylight in insects: a survey of ommatidial specializations in the dorsal rim area of the compound eye. *Microsc. Res. Tech.* 47, 368–379.
- Labhart, T., Hodel, B., Valenzuela, I., 1984. The physiology of the cricket's compound eye with particular reference to the anatomically specialized dorsal rim area. *J. Comp. Physiol. A* 155, 289–296.
- Labhart, T., Meyer, E.P., Schenker, L., 1992. Specialized ommatidia for polarization vision in the compound eye of cockchafers, *Melolontha melolontha* (Coleoptera, Scarabaeidae). *Cell Tissue Res.* 268, 419–429.
- Pomozí, I., Horváth, G., Wehner, R., 2001. How the clear-sky angle of polarization pattern continues underneath clouds: full-sky measurements and implications for animal orientation. *J. Exp. Biol.* 204, 2933–2942.
- Reinecke, A., Ruther, J., Tolasch, T., Francke, W., Hilker, M., 2002. Alcoholism in cockchafers: orientation of male *Melolontha melolontha* towards green leaf alcohols. *Naturwissenschaften* 89, 265–269.
- Schneider, F., 1952. Untersuchungen über die optische Orientierung der Maikäfer (*Melolontha vulgaris* F. und *M. hippocastani* F.) sowie über die Entstehung von Schwärmbahnen und Befallskonzentrationen. *Mitt. Schweiz. Entomol. Ges.* 25, 269–340.
- Shashar, N., Cronin, T.W., Wolff, L.B., Condon, M.A., 1998. The polarization of light in a tropical rain forest. *Biotropica* 30, 275–285.
- Suhai, B., Horváth, G., 2004. How well does the Rayleigh model describe the E-vector distribution of skylight in clear and cloudy conditions? A full-sky polarimetric study. *J. Opt. Soc. Am. A* 21, 1669–1676.
- Umow, N., 1905. Chromatische Depolarisation durch Lichtstreuung. *Phys. Z.* 6, 674–676.
- Zufall, F., Schmitt, M., Menzel, R., 1989. Spectral and polarized light sensitivity of photoreceptors in the compound eye of the cricket (*Gryllus bimaculatus*). *J. Comp. Physiol. A* 164, 597–608.